# AN EXPERIMENTAL STUDY OF AIR-WATER POOL ENTRAINMENT IN HIGH GAS FLUX REGION

**Peng Zhang[1], Peipei Chen[2], Wei Li[1], Zhi Di[1], Lei Zhang[1], Xiao Hu[1], Yaheng Zou[1]**

1. State Nuclear Power Technology R&D Center
Future S&T City, Changping, Beijing, China

2. State Nuclear Power Technology Corporation
North Road of 3rd Circle, Beijing, China

zhangpeng5@snptc.com; chenpeipei@snptc.com.cn; liwei5@snptc.com;
dizhi@snptc.com;zhanglei3@snptc.com; huxiao@snptc.com; zouyaheng@snptc.com

## ABSTRACT

Pool entrainment is an important phenomenon in LOCA transient in both conventional and passive PWR plants. Kataoka & Ishii pool entrainment model is widely used in small break LOCA and reactor transient analysis, but has limited validation against experimental data in high gas flux region. This paper is to report an experimental study of air-water pool entrainment with prototypic gas flux conditions of AP1000.The test section is 2200 mm long and 380 mm in diameter, and built by transparent material for visualization. The range of air flow superficial velocity is 0.98-5.41 m/s. The two phase mixture level is measured by Guided Wave Radar (GWR), and the water entrainment is recorded by weight measure after it is separated from entrainment separator. A correlation of pool entrainment in high gas flux region is proposed based on experimental data obtained in this study. The phenomenon of entrainment saturation is found in high gas flux region. The visualization indicates that pool entrainment in high gas flow region is in transition to jet/fountain flow, which might has strong exit effect.

## 1. INTRODUCTION

Entrainment from a liquid pool by gas flow in boiling or pool entrainment is recognized as an important phenomenon in nuclear engineering system. In conventional Pressurized Water Reactors (PWR), pool entrainment plays an important role in boric acid concentration balance in long term core cooling analysis. For advanced passive PWR, such as AP1000, pool entrainment is one of key phenomena in small break LOCA analysis. Existing safety analysis codes are reported to have limited capability in modeling pool entrainment in upper plenum after Automatic Depressurization System (ADS) is actuated [1, 2]. Other modern PWR design, such as APR1400, has adopted Safety Depressurization System (SDS) to rapidly depressurize reactor primary system in case of events beyond the design basis accidents. Pool entrainment through SDS valve at the top of pressurizer has significant impact on liquid discharge and two phase swelling during depressurization transient [3].

The most referenced pool entrainment model is developed by Kataoka [4], and is widely used in safety analysis codes [1-3]. Kataoka proposed three regions in pool entrainment mechanism and modeled them

differently: (a) near surface region, (b) momentum controlled region, and (c) deposition controlled region. For each region, the statistical total entrainment rate $E_{fg}$ is characterized as a function of gas superficial velocity, two phase mixture level, vessel diameter and fluid properties.
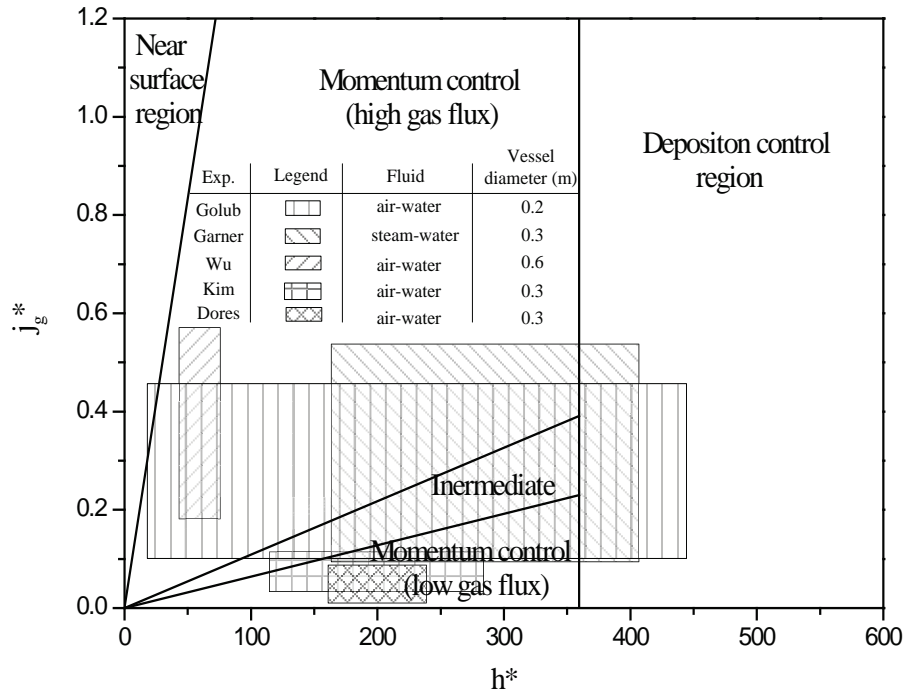


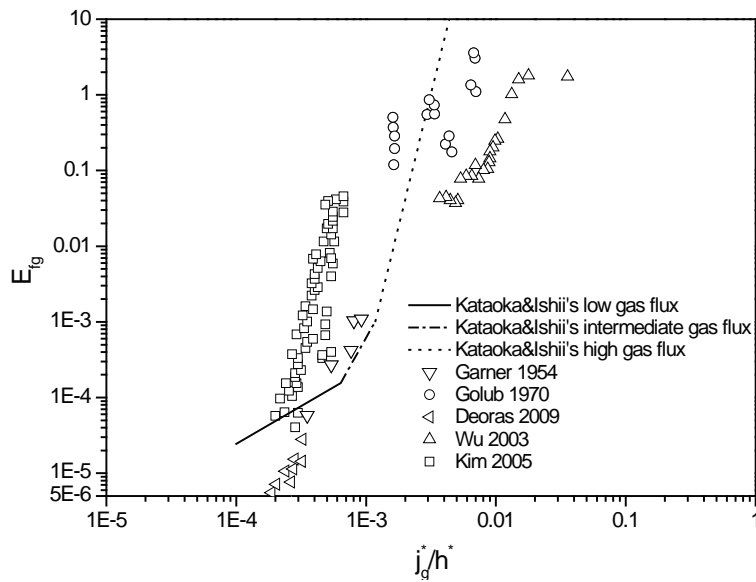**Figure 1. Pool Entrainment Experimental Data in Literature**



**Figure 2. Existing Data vs. Kataoka & Ishii Model**

Figure 1 illustrates pool entrainment experimental data obtained at atmospheric pressure in literature.

Results from Garner [5] and Golub [6] were used by Kataoka and Ishii to develop their model. Most of experiments were conducted at conditions with $j_g^*$, the non-dimensional form of gas superficial velocity, less than 0.5, or with air/steam superficial velocity less than 2.5 m/s approximately. However, in a typical AP1000 SBLOCA accident with double-ended DVI line breaks, the steam superficial velocity at upper plenum, where pool entrainment occurs, will stay in the range of 2.5-10 m/s for a few hours. Due to the lack of available data at high gas flux region, Kataoka only suggested a proportional relationship of a power function in the ratio of superficial gas velocity and height above two phase mixture surface.

$$E_{fg} \propto (j_g^* / h^*)^{7 \sim 20} \tag{1}$$

Therefore, more experimental data at high gas flux is needed for pool entrainment modeling or to complete the empirical correlation like Equation 1.

Some recent experimental studies are reported by Wu [2], Kim [3] and Deoras [6] with more advanced instrumentation and better documentation. Test sections used in above experiments have specific outlet features, which are chosen to simulate prototypic engineering design. For instance, test sections in Kim [3] and Deoras [6] have reduced area at outlet, which may result in strong Bernoulli effects at top of test section and cause higher gas velocity and entrainment rate. Wu conducted pool entrainment test at ATLATS facility with flow outlet at side of test section to reflect the geometry configuration of reactor upper plenum and hot leg, which may result in lower entrainment rate. Therefore, as shown in Figure 2, experiment data from Wu [2], Kim [3] and Deoras [6] shows some level of deviation from the predictions by Kataoka&Ishii's model.

This paper is to report an experimental study of pool entrainment at high gas flux, of which data is scarce in literature. Analysis of two phase mixture level instrumentation used in experiment is also provided. Experiment results are discussed, and an empirical correlation is proposed for pool entrainment rate of high gas flux region.

## 2.  EXPERIMENT APARATUS AND INSTRUMENTATION

### 2.1. Experiment Set-up

The schematic diagram of the experiment facility is shown in Figure 3.  The test facility include air supply system, water supply system, test section, entrainment separator, water entrainment collect tank, instrumentation and data acquisition system.

The air blower is able to supply air flow at maximum volumetric flow rate about **37 m³/min**, which corresponds to a superficial gas velocity $j_g$= **5.5m/s** in the test section and dimensionless superficial gas velocity $j_g^* \approx$**1.1**. The air flow rate can be adjusted by the inverter of air blower and a bypass loop. Two independent air supply lines are designed for high/low air flow demands.

Deionized water is prepared in the injection tank and the storage tank before experiments. The flow rate of supplied water to the injection tank can be controlled by a bypass loop between the injection tank and the storage tank. Water is injected from the bottom of the test section, thus the injection tank and the test section have the same collapsed water level at all times. The injection tank is supported by a lift which gives more flexibility to control the water level if necessary.

In order to have a uniform air flow, an air inlet distributor is installed at the bottom of the test section as shown in Figure 3. Air enters the test section through about 300 holes with 5mm in diameter, while water

enters the test section through 37 pipes with 20mm in diameter. The test section, shown in Figure 4, is **0.38m** in diameter and **2.2m** in height, and made by PMMA transparent material for visualization.

Figure 5 illustrates the air/entrainment separator installed on the top of the test section. The separation efficiency of the air/entrainment separator is more than 99.99%. Three glass windows are installed at the side of the test section for visualization. The entrainment water is collected and weighted in entrainment collect tank. The maximum weight measure capacity is 2000kg with an uncertainty of 2‰.
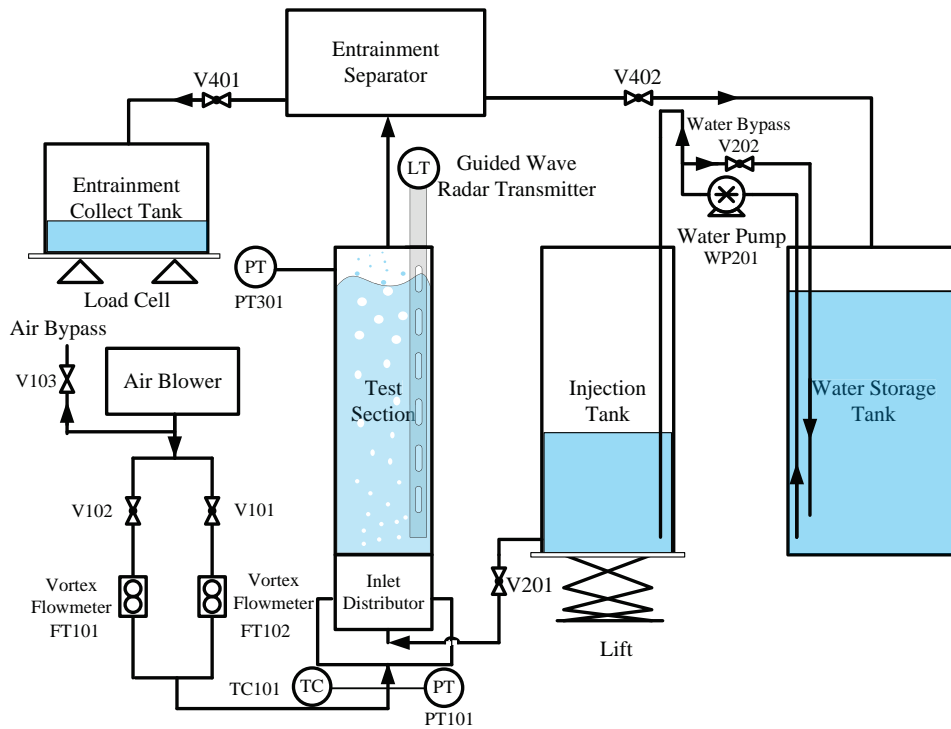


**Figure 3. Schematic Diagram of Experiment Apparatus**



**Figure 4. Air Inlet Distributor and Test Section**
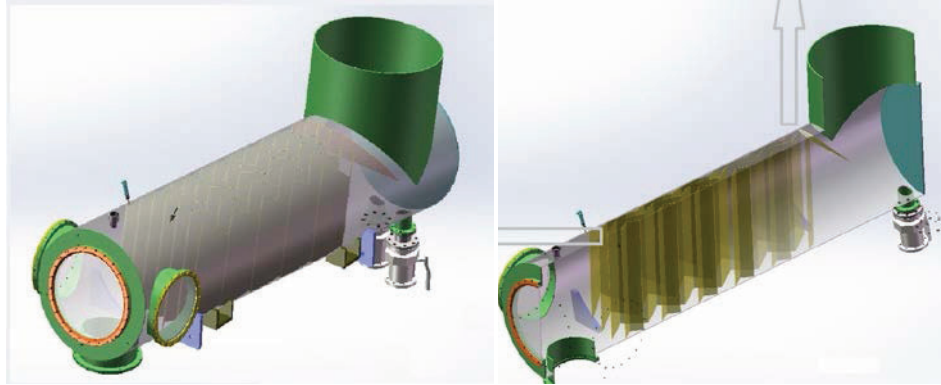
**Figure 5. Air/Entrainment Separator**

## 2.2 Instrumentation and Data Uncertainty

Pressure and temperature are measured at the inlet and outlet of the test section respectively. All temperatures are measured by Type K thermocouple with an uncertainty of $\pm 1^{\circ}$C. The air flow is measured by two vortex flow meters with an uncertainty of $\pm 0.5\%$. The weight of entrainment collect tank is measured by 3 load cell with an uncertainty of $\pm 4$kg. The location of the pool surface (two phase mixture level) is measured by a Guided Wave Radar (GWR) made by Magnetrol® (Model 706) with a static uncertainty of $\pm 2.5$mm. The radar probe is installed at the center of the test section as shown in Figure 4. All measurements are recorded by NI® data acquisition system.

In Kataoka's model, one of the key parameters that characterize pool entrainment rate is the two phase mixture level. Therefore, extra attention is paid to examine the accuracy and uncertainty of the two phase mixture level measurement. Guided Wave Radar uses deflective electromagnetic pulse from dielectric discontinuity interface to locate the pool surface, which has been widely used in chemical industry to measure liquid level in a variety of storage tanks since 2000. But in most of industry applications, Guided Wave Radar is to measure the stratified two phase interface. To the best knowledge of authors, no calibration data is available for the dynamic characteristic of Guided Wave Radar in measuring churn-turbulent two phase mixture surface as conditions of this study. Thus, a visualization system is used to study the dynamic accuracy and uncertainty of Guided Wave Radar measurement.

Figure 6 shows the measurements by Guided Wave Radar and visualization for a moving stratified two phase interface (a decreasing pool surface without air injection). It can be found that the measurement by Guided Wave Radar is approximately 2 seconds behind the camera (50Hz). If compensating a 2-seconds offset, the measurement is within 2.5mm uncertainty range provided by Magnetrol® user's manual.
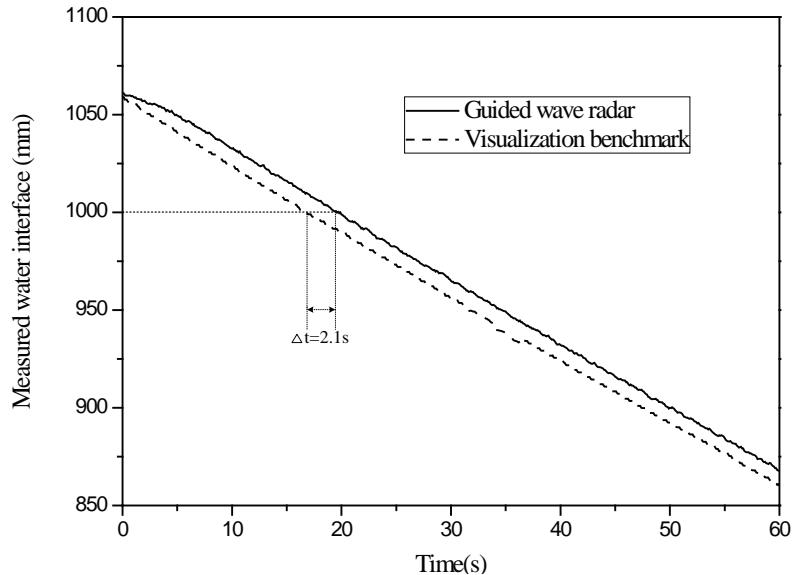
**Figure 6.Calibration of Guided Wave Radar on a Moving Stratified Two Phase Interface**

In order to detect the churn-turbulent pool surface level (two phase mixture level) in images like the left picture in Figure 7, a LABVIEW program is developed to convert the original image to a binary image like the right picture in Figure 7 for image processing. The program is able to identify the boundary of two phase mixture and calculate its width in each binary image. It can be found that the width of two phase mixture decreases and finally disappears at vertical direction. Therefore, the churn-turbulent pool surface may be defined by two phase mixture width ratio $r = l / L$ as shown in Figure 8. At this moment, a value of 0.8 is used to identify the churn-turbulent pool surface.

Figure 9 demonstrates churn-turbulent pool surface levels (two phase mixture level) obtained by Guided Wave Radar and visualization method. It is clear that the magnitude of fluctuationin pool surface level provided by Guided Wave Radar is much smaller than visualization method (approximately $\pm 15$mm vs. $\pm 90$mm), while the statistical averages of pool surface from both methods are relatively close (611.9mm vs.622.5mm). This indicates that the pool surface is fairly agitated, but the time response characteristic of Guided Wave Radar is so slow that it is not able to capture the fast movement of the two phase mixture level at high gas flux region. This observation is consistent with the findings in the calibration data shown in Figure 6 that measurement from Guided Wave Radar is always about 2 seconds behind benchmark data. Except for low capability tracing agitating pool surfaces, Guided Wave Radar is still able to provide reasonable good statistical average value of two phase mixture level. If visualization data is chosen as benchmark, the uncertainty of two mixture level data (time averaged) by Guided Wave Radar is about $\pm 10$mm.

Based on measurement uncertainty of air flow meter, Guided Wave Radar and load cells discussed above, the uncertainty of $j_g^*/h^*$ and $E_{fg}$ for a typical test results ($j_g^*/h^* \approx 0.002$ and $E_{fg} \approx 1$) is $\pm 1.4 \times 10^{-5}$ and $\pm 0.0227$, respectively. The uncertainty of $j_g^*/h^*$ and $E_{fg}$ is well captured by the size of symbol used in Figure 10.
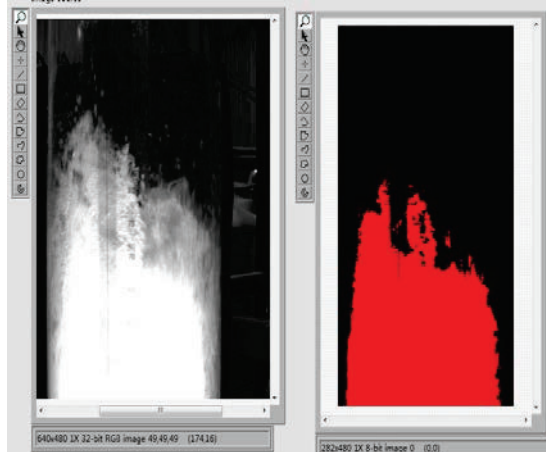
**Figure 7. Image Processing of Churn-turbulent Pool Surface
(Left: original image, Right: processed image)**
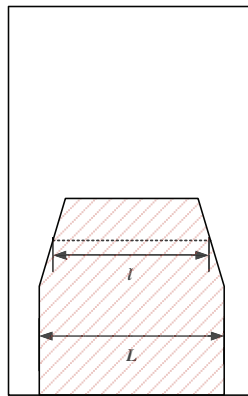


**Figure 8. A Simplified Binary Image of Churn-turbulent Pool Surface**
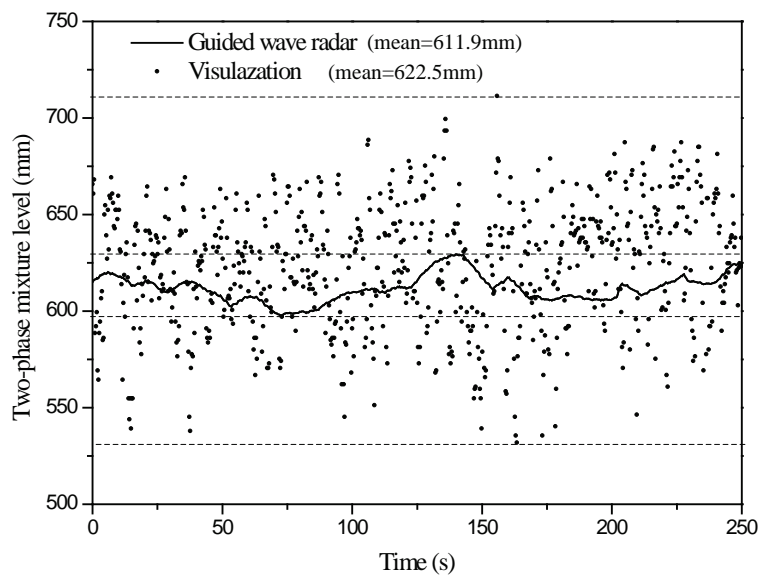


**Figure 9. Measurement of Churn-turbulent Pool Surface Level ($j_g$= 3.9m/s)**

## 2.3 Test Conditions

The experiments are carried out under atmosphere pressure and room temperature (approximately 20$^{\circ}$C). In Kataoka's model, the entrainment rate is characterized by the ratio of two non-dimensional parameters, $j_g^*/h^*$, for given pressure and temperature. Total of 43 tests are performed under wide range of air flow and two phase mixture level conditions, which are illustrated in Table I.

**TableI. Experiment Conditions of Major Parameters**

| Air flowrate (m$^3$/min) | $j_g$(m/s) | $j_g^*$ | $h$(m) | $h^*$ | $j_g^*/h^*$ | Number of Data Set |
|---|---|---|---|---|---|---|
| 6.67~36.8 | 0.98~5.41 | 0.21~1.16 | 0.187~1.53 | 66.8.~541.2 | 0.0015~0.0063 | 43 |

## 2.4 Test Procedure

All experiments are conducted at steady state condition. For a given air flow rate, two phase mixture level in test section can be controlled by adjusting liquid supply line bypass valve (V202). Data will be recorded once the steady two phase mixture level is achieved at given air flow rate. The minimum data recording time is 300 seconds. For test conditions with low entrainment rate, recording time will be extended in order to reduce data uncertainty of weight measurement of entrainment collect tank.

## 3. RESULTSAND DISCUSSION

The results of current study are shown in Figure 10 with other pool entrainment experimental data available in literature. All test data are plotted against predictions by Kataoka's model (line 1-4) using air physical properties at atmospheric pressure and 20$^{\circ}$C. Line 1-4 respectively represent low, intermediate, high gas flux and near surface region defined in Kataoka's model. It can be seen that current data agrees with Kataoka' model reasonably well in high gas flux region. Kataoka suggests a power function relationship between entrainment rate and the ratio $j_g^*/h^*$ with power parameter of 7~20 in high gas flux region, (see Equation 1). If one takes the format as Equation 1, the following correlation gives the best fitting to current data.

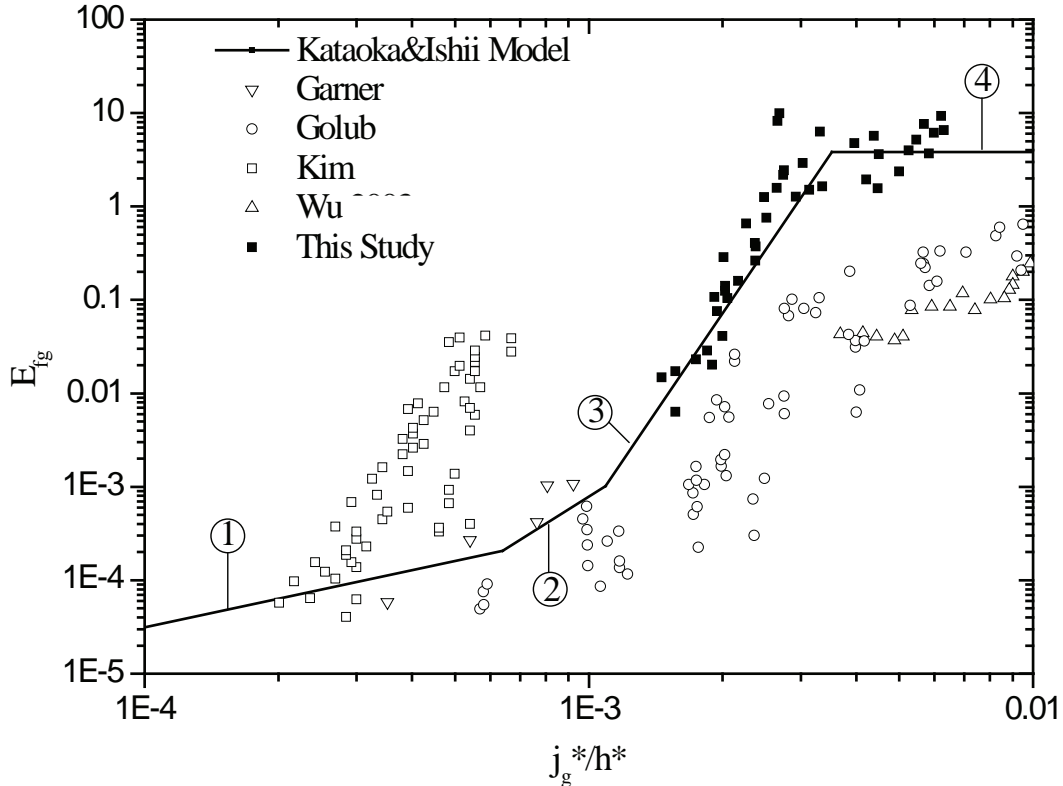$$E_{fg} = 4.0 \times 10^{19} (j_g^*/h^*)^{7.6}$$  (2)

**Figure 10. Comparison of Current Data with Model Prediction and Existing Data**

In Figure 10, data from Wu [2] and Golub [6] are also presented because their experiments were conducted at similar $j_g^*/h^*$ range as this study. Attention needs to be paid to the fact that, as shown in Figure 11, Wu and Golub performed their tests at low gas flow and high two phase mixture level (small distance above two phase mixture surface), while this study has most of experiment points at higher gas flow and lower two phase mixture level (big distance above two phase mixture surface).

As discussed in early section, ATLATS facility used by Wu has side exit at the top of the test section to reflect the geometry of the reactor upper plenum and the hot leg, which may result in lower entrainment rate. Kataoka's model, however, assumes the top outlet of gas flow at space above the two phase mixture surface, and does not account for impact of gas flow right-turn (or left-turn) on liquid entrainments. Authors cannot find the reference [6], therefore the test section configuration used by Golub is not clear. Nevertheless, it is reasonable to assume certain degree of exit effect on pool entrainment.

In addition, data shown in Figure 10 indicates that entrainment rate deviates from the power function with high $j_g^*/h^*$. For the current data, entrainment rate seems to reach "saturation" (entrainment is decoupled from $j_g^*/h^*$) when $j_g^*/h^*$ is larger than $2 \times 10^{-3}$. Similar trend can also be observed in Wu's and Golub's data in Figure 10. The phenomenon that entrainment is independent of $j_g^*/h^*$ is also reported at "near surface region" by Kataoka (Equation 3 and 4). However, the "saturation region" presented in Wu, Golub and current study is NOT the "near surface region" because the value of $h^*$ in Wu, Golub and current study is much larger than threshold value (in the magnitude of 0.01) calculated by Equation 3 for air at atmospheric condition.

$$0 \le h^* \le 1.308 \times 10^3 j_g^* N_{\mu g}^{0.5} D_H^{*0.42} (\frac{\rho_g}{\Delta \rho})^{0.23} \tag{3}$$

$$E_{fg} = 4.84 \times 10^{-3} \left( \frac{\Delta \rho}{\rho_g} \right) \tag{4}$$

The entrainment rate at near surface region is **3.84** in conditions of this study, which is, interestingly, very close to the statistic average of entrainment rate in "high gas flux entrainment saturation region" as shown in Figure 10. Kataoka [4] reckons that "Measuring the entrainment amount in this region (near surface region) is difficult because the pool surface is highly agitated. Therefore, the discrimination of entrained droplets from the agitated pool is quite difficult". Similar phenomena can be observed in high gas flux region with high $h^*$ value (larger than near surface region threshold value). Figure 13 shows agitated entrainment liquid (like pseudo jet or fountain flow) at the test section exit in high gas flux condition, which indicates a clear flow regime transition from churn-turbulent that is normally observed intermediate gas flow regime [3, 7].
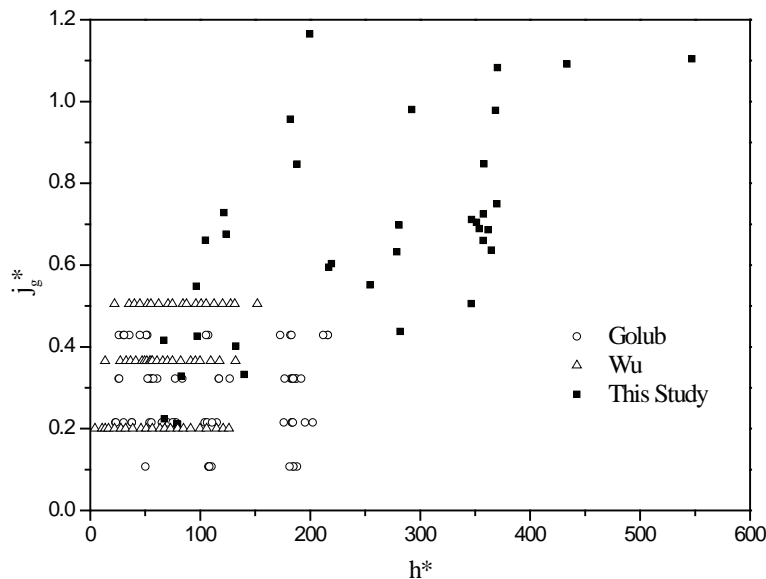


**Figure 11. Comparison of Test Condition of This Study with Golub [6] and Wu [2]**

Figure 12 re-plots current data that are near Line-4 in Figure 10 (entrainment saturation region) in a $j_g^*$-$h^*$ diagram. The linear fitting of those entrainment saturation points gives a slop of $5.88 \times 10^{-3}$. Thus, all shaded area in Figure 12, which can be denoted by the following equation, is in entrainment saturation region.

$$j_g^* / h^* \geq 5.88 \times 10^{-3} \tag{5}$$

Wu's and Golub's entrainment data also indicate phenomena of entrainment saturation at high gas flux as shown in Figure 10. If one collects those data points and plot them in Figure 12, they are in entrainment saturation region defined by Equation 5.

High gas flux or entrainment saturation region normally comes with very agitated two mixture level as indicated in Figure 9, pseudo jet/fountain type of flow is very common as shown in Figure 13. Sometimes, the jet flow is so substantial that it is difficult to differentiate the liquid entrainment from the overflow. In the interests of engineering application that pool entrainment may occur, the vessel outlet where gas and entrainment escape usually has unique structure (i.e. entrainment to top exit with reduced area in SDS valve in APR1400 and entrainment from upper plenum to hot leg in AP1000). If velocity or direction of gas flow has significant change at vessel outlet, extra attention needs to be paid to compensate the exit effect on pool entrainment correlation developed in this study.
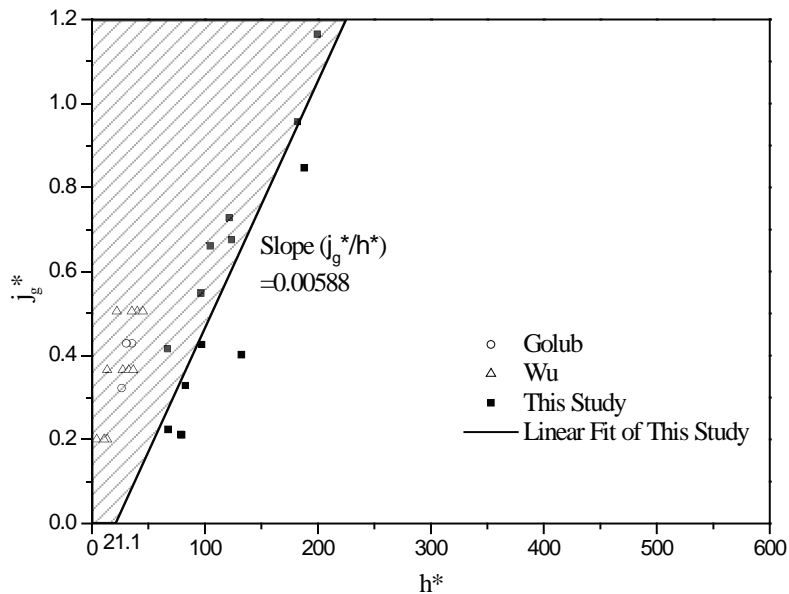


**Figure 12. Entrainment Saturation Region**



**Figure 1. Transition to Pseudo Jet/Fountain Flow at High Gas Flux Conditions**

## 4. CONCLUSION AND PROSPECTS

Air/water pool entrainment experiments are conducted at atmosphere pressure with high gas superficial velocity (0.98~5.41m/s). The uncertainty of Guided Wave Radar that measures two phase mixture level is analyzed by benchmarking with visualization results. An image processing program is developed to detect

pool surface on images recorded by visualization. It is found that Guided Wave Radaris not able to trace fast movement of thetwo phase mixture level, but has reasonable accuracy on statistic average of two phase mixture level with uncertainty of 10mm at typical test conditions in this study. Total 43 sets of pool entrainment data are collected at various combinations of gas flux and two phase mixture level. A correlation of pool entrainment at high gas flux region is proposed based on Kataoka's model and current data. It is found that current data has higher entrainment rate than early experimental results by Wu [2] and Golub [6]. It is believed that entrainment exit effect is the potential cause for such deviation. A phenomenon of entrainment saturation is found at high gas flux region in which liquid entrainment is independent of gas flux and two phase mixture level. A mathematical equation is proposed to give a criterion of entrainments saturation.

The visualization of pool entrainment indicates a strongly agitated two phase mixture level at high gas flux, and a transition from churn-turbulent flow to pseudo jet/fountain flow is observed in this study. The use of statistic average of two phase mixture level to characterize pool entrainment has undeniable shortcomings at high gas flux region because it ignores important information of pool surface fluctuation. The challenge may be even more difficult to overcome at pseudo jet/fountain flow conditions such that the "two phase mixture level" might be neither applicable nor measurable. Although this study provides some practical convenience to engineering analysis that involves pool entrainment, a more fundamental model is needed to fully characterize the physical behavior of pool entrainment at high gas flux region. At the end, it is desired that more studies can be done to give a quantitative understanding of exit effect on pool entrainment.

## NOMENCLATURE

| | |
|---|---|
| $D_H$ | Hydraulic diameter of vessel |
| $D_H{}^*$ | Dimensionless hydraulic diameter of vessel defined as $D_H / \sqrt{\sigma / g\Delta\rho}$ |
| $E_{fg}$ | Entrainment defined as $\rho_f j_f / \rho_g j_g$ |
| $G$ | Acceleration due to gravity |
| $h$ | Height above the pool surface |
| $h^*$ | Dimensionless height above the pool surface defined as $h / \sqrt{\sigma / g\Delta\rho}$ |
| $j_f$ | Superficial liquid velocity |
| $j_g$ | Superficial gas velocity |
| $j_g{}^*$ | Dimensionless superficial gas velocity defined as $j_g /(\sigma g\Delta\rho / \rho_g^2)^{1/4}$ |
| $N_{\mu g}$ | Gas viscosity number defined as $\mu_g /(\rho_g \sigma \sqrt{\sigma / g\Delta\rho})^{1/2}$ |
| $\Delta\rho$ | Density difference between gas and liquid |
| $\rho_f$ | Density of liquid |
| $\rho_g$ | Density of gas |
| $\sigma$ | Surface tension |

## REFERENCES

1.  AP1000 Design Control Document, Revision 19, 15.6-31
2.  Q. Wu, P. Young, K. Abel, Y. Yao, Y.J.Yoo, K.B. Welter , S. M. Bajorek, J. Han, "Liquid Entrainment in Reactor Vessel", *13th International Conference on Nuclear Engineering*, Beijing, China(2005).
3.  C. H. Kim, H. C. No, "Liquid entrainment and off-take through the break at the top of a vessel", Nuclear Engineering and Design, **235,** pp.1675–1685(2005).
4.  I. Kataoka, M. Ishii, "Mechanistic Modeling and Correlations for Pool Entrainment Phenomenon", *NUREG/CR-3304*(1983).
5.  F.H. Garner, S.R.M. Ellis, J.A. Lacey, "The Size Distribution and Entrainment of Droplets", *Trans. Inst. Chem, Engs*. **32**(222)(1954).
6.  S.I. Golub, "Investigation of Moisture Carryover and Separation in Evaporation Apparatus", *Candidates Dissertation*, MEI(1970) (quoted from refer. [4]).
7.  M. P.Deoras, Z. M.Rahul, N. I.Kannan, "Experiment Study of Liquid Carryover in Separator Drum", *Nuclear Engineering and Design,* **240**, pp.76-83(2010).